Acta Scientific Pharmaceutical Sciences (ISSN: 2581-5423)

Volume 7 Issue 7 July 2023

Research Article

Development, Synthesis and Antiprotozoal Assessment of New Substituted Diquinolinyl-Pyridine Derivatives as Antiparasitic Agents by Potential G-4 Binding

Rabindra Nath Das[1,2], Anita Cohen[3], Clotilde Boudot[4], Solène Savrimoutou[1], Sandra Albenque-Rubio[1], Stéphane Moreau[1], Jean-Louis Mergny[5], Luisa Ronga[6], Ioannis Kanavos[6], Charles Descamps[1], Valentin Verdier[1], Patrice Agnamey[7], Catherine Mullié[7], Bertrand Courtioux[4], Pascal Sonnet[7] and Jean Guillon[1]*

[1]University of Bordeaux, Faculty of Pharmacy, CNRS, INSERM, ARNA, France

[2]Department of Chemistry, College of Engineering and Technology, Kattankulathur – Chennai, Tamil Nadu, India

[3]University of Aix-Marseille, IRD, AP-HM, SSA, VITROME, France

[4]University of Limoges, INSERM U1094, Tropical Neuroepidemiology, Limoges, France; Institute of Neuroepidemiology and Tropical Neurology, France

[5]Ecole Polytechnique, Laboratoire d'Optique et Biosciences, CNRS, INSERM, Institut Polytechnique de Paris, France

[6]Université de Pau et des Pays de l'Adour, E2S UPPA, CNRS, IPREM, France

[7]University of Picardie Jules Verne, Agents Infectieux, Résistance et Chimiothérapie (AGIR), UR 4294, UFR de Pharmacie, France

***Corresponding Author:** Jean Guillon, University of Bordeaux, Faculty of Pharmacy, CNRS, INSERM, ARNA, France.

DOI: 10.31080/ASPS.2023.07.0965

Received: May 16, 2023

Published: May 23, 2023

Abstract

In order to fight malaria, a public health problem for which nearly half of the world's population is at risk and responsible a life-threatening disease primarily found in tropical countries and for which the estimated number of deaths stood at 619 000 in 2021, an original strategy is to design and synthesize quinoline-based drugs that are not recognized by the protein system involved in the drug efflux. Thus, a series of new 2,6-di-(carbamoyl-2-quinolinyl)pyridine derivatives was considered, synthesized, and evaluated *in vitro* against three parasites (*Plasmodium falciparum*, *Leishmania donovani* and *Trypanosoma brucei brucei*). Pharmacological results showed antiparasitic activity with IC_{50} values in the sub and µM range. The *in vitro* cytotoxicity of these new diquinolinyl-pyridine derivatives was evaluated on human HepG2 cells. The diquinolinyl-pyridine 1e was found as the most potent antimalarial candidate with a ratio of cytotoxic to antiprotozoal activities of 73.5 against the *P. falciparum* CQ-resistant strain W2. Moreover, derivative 3b was also identified as the most potent antiparasitic compound with a selectivity index (SI) of 21.48 on 3D7 *P. falciparum* CQ-sensitive strain. In addition, the 2,6-di-(carbamoyl-2-quinolinyl)pyridines 2c and 3b were also identified as the most interesting antitrypanosomal candidate drugs with selectivity index (SI) of 75.9 and 38.94, respectively on *T. brucei brucei* strain. It has been previously described that the telomeres of parasites *P. falciparum* and Trypanosoma could be considered as potential targets of this kind of nitrogen heterocycles, thus the ability of these new derivatives to stabilize the parasitic telomeric G-quadruplexes have been measured through a FRET melting assay.

Keywords: Diquinolinyl-pyridine; Antimalarial Activity; Antileishmanial Activity; Antitrypanosomal Activity; G-quadruplex.

Introduction

In 2021, there were an estimated increase of 2 million malaria cases worldwide, since 247 million cases have been recorded compared to 245 million in 2020 according to the last WHO Malaria report [1]. Nowadays, nearly half of the world's population is at risk of malaria, in particular pregnant women and young children. In this context, in 2022, the WHO published guidance on new recommendations which were last updated on March 14th, 2023 [2]. Even with the remarkable efforts during the COVID-19 pandemic to maintain services, malaria control efforts face many health system challenges such as long-term humanitarian crisis and the undoubtable influence of climate change on the spread of this worrying disease. In Africa notably, the invasion by Anopheles stephensi, a mosquito able to adapt easily to urban environments, poses a real risk of public health, in addition to the growing problems of resistance to insecticide-treated nets and to antimalarial drugs. Furthermore, these difficulties impact the control of all vector-borne neglected tropical diseases, such as leishmaniasis and trypanosomiasis (Chagas disease and human African trypanosomiasis) as well [3]. By the way, a global strategy was proposed by WHO in "Ending the neglect to attain the sustainable development goals: a road map for neglected tropical diseases 2021-2030" [4] prepared through a global consultation worldwide. In this context, "research and innovation are fundamental enablers of programmatic progress for all (neglected) tropical diseases". It seems essential to integrate and improve cross-cutting approaches, such as new treatments approaches and investigation of a community-based and applied research for several of these tropical diseases.

Thus, an another original strategy is to design and synthesize quinoline-based drugs that are not recognized by the protein system involved in the drug efflux, such as primaquine (PQ) or amodiaquine (AQ). The efflux pumps serve both as natural defense mechanisms and influence the bioavailability and disposition of drugs. Initially, such mechanism was suggested in *Plasmodium falciparum* where erythrocytes infected with CQ resistant parasites accumulated significantly less drug than the sensitive ones, before its further study led to the identification of the Pfcrt gene among other quinoline drug resistance mechanisms. Such new series that have been not recognized by the protein system involved in the drug efflux of bisquinoline A and bisacridine B antimalarial drugs (Figure 1, compounds A-B and Piperaquine) have been described in the literature [5-10]. These new derivatives had much lower resistance indices than CQ, indicating that these bis-heterocyclic structures are less efficiently rejected by efflux by drug-resistant parasites. Recently, the promising new derivative cabamiquine (DDD-107498), a quinoline-4-carboxamide, was discovered with activity against multiple life-cycle stages of the parasite. It showed a novel mechanism of action by inhibition of translation elongation factor 2 (PfEF2), which is a crucial step for protein synthesis [11,12]. Another series involving quinoline-4-carboxamide moiety were also investigated leading to derivative C showing promising antiplasmodial activity [13].

During our work focused on the discovery of new nitrogen heterocyclic derivatives that can be used in antiprotozoal chemotherapy [14-20], we have previously developed various series of bis[(substituted-aminomethyl)phenyl]azahetrocycles, which could bind to *Plasmodium falciparum* DNA G-quadruplexes [15,18,20] in order to bypass the resistance mechanisms developed by the parasites and based on efflux. By considering our experience in the field of the synthesis of new antiprotozoal heterocyclic derivatives, we describe here the design and synthesis of new 2,6-di-(carbamoyl-2-quinolinyl)pyridines salts 1-3 (Figure 1), in which two quinoline-carboxamide groups are linked to a pyridine nucleus. These novel derivatives 1-3 could be considered as original bis bio-isoster analogs of the previously described potent antimalarial cabamiquine, in order to increase their antiprotozoal activities.

We report on their *in vitro* antiplasmodial activity against the chloroquine-sensitive (3D7) and the chloroquine-resistant (W2) strains of the malaria parasite *P. falciparum*. As aza heterocyclic pharmacophores are the fundamental units of many antiprotozoan candidates, these novel quinoline-like derivatives were also tested for *in vitro* efficacy against medically important protozoans *Leishmania donovani* and *Trypanosoma brucei brucei*.

In addition, the *in vitro* cytotoxicity of our new substituted diquinolinyl-pyridine derivatives 1-3 was assessed in human HepG2 cells, and an index of selectivity, the ratio of cytotoxic to antiparasitic activity, was determined for each derivative. The telomeres of the different protozoa could constitute potential

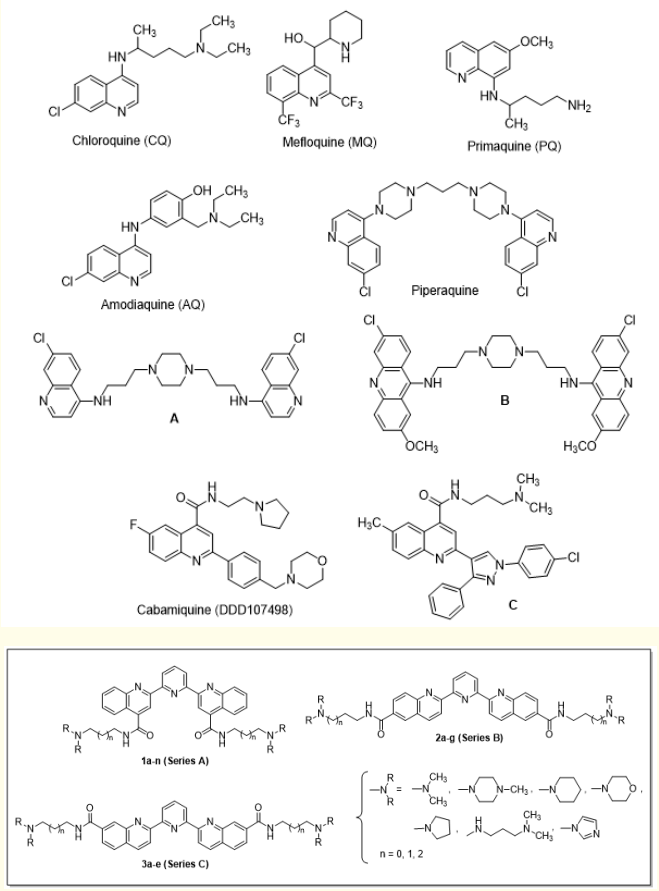

Figure 1: Chemical structures of chloroquine, mefloquine, primaquine, amodiaquine, piperaquine, bisquinoline A, bisacridine B, cabamiquine, quinoline C and new substituted diquinolinyl-pyridine derivatives 1-3.

attractive drug targets [21-24] in order to bypass the problem of resistance mechanisms based on efflux, it has been previously described that telomerase activity is detected in gametocytes and during the transition to the erythrocytic stage of *P. falciparum* [25]. The telomeric 3' G-overhang region of *P. falciparum* is a repetition of degenerate unit 5'GGGTTYA3' (where Y could be T or C) [26] which can fold into intramolecular G-quadruplex [27]. This difference between parasitic and human (5'GGGTTA3') G-quadruplexes is also observed with L. spp and *T. brucei brucei*, which augurs the possibility of developing antiparasitic ligands targeting specifically G-quadruplexes found in these protozoal species. Thus, we investigated whether some promising bioactive compounds could stabilize some parasitic telomeric DNA G-quadruplex structures. Thus, potential stabilization of *P. falciparum* and *T. brucei brucei* telomeric G-quadruplexes was evaluated using a FRET melting assay.

Materials and Methods

Chemistry

Commercially available reagents were used as received without additional purification. Melting points were determined with an SM-LUX-POL Leitz hot-stage microscope (Leitz GMBH, Midland, ON, USA) and are uncorrected. NMR spectra were recorded with tetramethylsilane as an internal standard using a BRUKER AVANCE 300 spectrometer (Bruker BioSpin, Wissembourg, France). Splitting patterns have been reported as follows: s = singlet; bs = broad singlet; d = doublet; t = triplet; q = quartet; dd = double doublet; qt = quintuplet; m = multiplet. Analytical TLC were carried out on 0.25 precoated silica gel plates (POLYGRAM SIL G/UV254) and visualization of compounds after UV light irradiation. Silica gel 60 (70–230 mesh) was used for column chromatography. Mass spectra were recorded on an ESI LTQ Orbitrap Velos mass spectrometer (ThermoFisher, Bremen, Germany). Ionization was performed using an Electrospray ion source operating in positive ion mode with a capillary voltage of 3.80 kV and capillary temperature of 250 °C. The scan type analyzed was full scan, all MS recordings were in the m/z range between 150 and 2000 m/z. Elemental analyses were found within ±0.4% of the theoretical values. Diquinolinyl-pyridines 1b, 1e, 1h, 1j, 1l-m were synthesized as previously described in reference [27].

General procedure for the synthesis of 2,2'-(pyridine-2,6-diyl) bis(N-((substituted-amino)alkyl)quinoline-4-carboxamide) 1a, 1c-d, 1f-g, 1i, 1k, 1n, 2,2'-(pyridine-2,6-diyl)bis(N-((substituted-amino)alkyl)quinoline-6-carboxamide) 2a-g and 2,2'-(pyridine-2,6-diyl)bis(N-((substituted-amino)alkyl) quinoline-7-carboxamide) 3a-e

To diacid 4 or 6 or 8 5 mL of $SOCl_2$ was added and the reaction mixture was refluxed for 2 h. Excess of $SOCl_2$ was evaporated and the mixture was dried under vacuum. Then, v arious substituted aminoalkylamines were added directly in excess amount (3 mL) to diacyl chloride 5 or 7 or 9 (0.5 mmol) under cold condition. The

reaction mixture was stirred at room temperature for 24 h. It was cooled and 10 mL of water was added and stirred for 10 min. If the precipitate appeared, then it was filtered, washed with water then petroleum ether, and dried. If precipitate did not appear, then it was extracted with dichloromethane and the organic layer was evaporated to get the final product 1, 2 or 3.

2,2'-(Pyridine-2,6-diyl)bis(N-(2-(dimethylamino)ethyl) quinoline-4-carboxamide) (1a)

Beige crystals (yield, 61%), mp = 170-172 °C; ^{1}H NMR δ (300 MHz, $CDCl_3$ and 10% MeOD) 8.88 (s, 2H, -CH), 8.76 (d, 2H, J = 7.80 Hz, -CH), 8.33 (d, 2H, J= 8.50 Hz, -CH), 8.24 (d, 2H, J= 8.50 Hz, -CH), 8.08 (t, 1H, J = 7.80 Hz, -CH), 7.84-7.77 (m, 2H, -CH), 7.70-7.61 (m, 2H, -CH), 3.68 (q, 4H, J = 6.90 Hz, $-CH_2$), 2.67 (t, 4H, J = 6.90 Hz, $-CH_2$), 2.33 (s, 12H, $-N(CH_3)_2$); ^{13}C NMR δ (100 MHz, $CDCl_3$) 169.54 (2C=O), 157.01 (C-2_{pyr} and C-6_{pyr}), 156.49 (2C-2_{qui}), 149.66 (2C-$8a_{qui}$), 144.01 (2C-4_{qui}), 139.54 (C-4_{pyr}), 131.51 (2C-6_{qui}), 131.33 (2C-8_{qui}), 129.19 (2C-7_{qui}), 126.61 (2C-3_{qui}), 125.93 (2C-$4a_{qui}$), 123.82 (C-3_{pyr} and C-5_{pyr}), 118.28 (2C-5_{qui}), 59.25 ($2NCH_2$), 46.36 ($2N(CH_3)_2$), 38.68 ($2NCH_2$); ESI-MS m/z $[M+H]^+$ Calcd for $C_{33}H_{36}N_7O_2$: 562.293, Found: 562.298.

2,2'-(Pyridine-2,6-diyl)bis(N-(4-(dimethylamino)butyl) quinoline-4-carboxamide) (1c)

Beige crystals (yield, 73%), mp = 157-159 °C; ^{1}H NMR δ (300 MHz, $CDCl_3$ and 10% MeOD) 8.79 (s, 2H, -CH), 8.70 (d, 2H, J = 7.80 Hz, -CH), 8.24 (d, 2H, J= 8.70 Hz, -CH), 8.23 (d, 2H, J= 8.70 Hz, -CH), 8.15 (t, 1H, J = 7.80 Hz, -CH), 7.86-7.78 (m, 2H, -CH), 7.70-7.63 (m, 2H, -CH), 3.57 (t, 4H, J = 7.10 Hz, $-CH_2$), 2.40 (t, 4H, J = 7.10 Hz, $-CH_2$), 2.21 (s, 12H, $-N(CH_3)_2$), 1.78-1.70 (m, 4H, $-CH_2$), 1.68-1.62 (m, 4H, $-CH_2$); ESI-MS m/z $[M+H]^+$ Calcd for $C_{37}H_{44}N_7O_2$: 618.356, Found: 618.431.

2,2'-(Pyridine-2,6-diyl)bis(N-(2-(4-methylpiperazin-1-yl) ethyl)quinoline-4-carboxamide) (1d)

Beige crystals (yield, 75%), mp = 180-182 °C; ^{1}H NMR δ (300 MHz, $CDCl_3$ and 10% MeOD) 8.80 (s, 2H, -CH), 8.69 (d, 2H, J = 8.10 Hz, -CH), 8.33 (d, 2H, J= 8.40 Hz, -CH), 8.24 (d, 2H, J= 8.40 Hz, -CH), 8.14 (t, 1H, J = 8.10 Hz, -CH), 7.83 (t, 2H, J= 8.40 Hz, -CH), 7.66 (t, 2H, J= 8.40 Hz, -CH), 3.70 (t, 4H, J = 6.90 Hz, $-CH_2$), 2.74 (t, 4H, J = 6.90 Hz, $-CH_2$), 2.71-2.48 (m, 16H, $-CH_{2pip}$), 2.26 (s, 6H, $-NCH_3$); ^{13}C NMR δ (100 MHz, $CDCl_3$) 169.88 (2C=O), 157.07 (C-2_{pyr} and C-6_{pyr}), 156.53 (2C-2_{qui}), 149.57 (2C-$8a_{qui}$), 144.56 (2C-4_{qui}), 139.58 (C-4_{pyr}), 131.62 (2C-6_{qui}), 131.10 (2C-8_{qui}), 129.18 (2C-7_{qui}), 126.63 (2C-3_{qui}), 125.88 (2C-$4a_{qui}$), 123.83 (C-3_{pyr} and C-5_{pyr}), 118.30 (2C-5_{qui}), 58.00 ($2NCH_2$), 55.97 ($4NCH_{2pip}$), 53.72 ($4NCH_{2pip}$), 46.62 ($2NCH_3$), 38.17 ($2NCH_2$); ESI-MS m/z $[M+H]^+$ Calcd for $C_{39}H_{46}N_9O_2$: 672.377, Found: 672.968.

2,2'-(Pyridine-2,6-diyl)bis(N-(4-(4-methylpiperazin-1-yl) butyl)quinoline-4-carboxamide) (1f)

Yellow crystals (yield, 69%), mp = 159-161 °C; ^{1}H NMR δ (300 MHz, $CDCl_3$ and 10% MeOD) 8.80 (s, 2H, -CH), 8.72 (d, 2H, J = 8.10 Hz, -CH), 8.24 (d, 2H, J= 7.80 Hz, -CH), 8.22 (d, 2H, J= 7.80 Hz, -CH), 8.19 (t, 1H, J = 7.80 Hz, -CH), 7.84-7.81 (m, 2H, -CH), 7.70-7.64 (m, 2H, -CH), 3.58 (t, 4H, J = 6.90 Hz, $-CH_2$), 2.48 (t, 4H, J = 6.90 Hz, $-CH_2$), 2.62-2.32 (m, 16H, $-CH_{2pip}$), 2.18 (s, 6H, $-NCH_3$), 1.78-1.68 (m, 8H, $-CH_2$); ^{13}C NMR δ (100 MHz, $CDCl_3$) 170.00 (2C=O), 156.99 (C-2_{pyr} and C-6_{pyr}), 156.45 (2C-2_{qui}), 149.55 (2C-$8a_{qui}$), 144.84 (2C-4_{qui}), 139.60 (C-4_{pyr}), 131.62 (2C-6_{qui}), 131.11 (2C-8_{qui}), 129.20 (2C-7_{qui}), 126.41 (2C-3_{qui}), 125.92 (2C-$4a_{qui}$), 123.77 (C-3_{pyr} and C-5_{pyr}), 118.10 (2C-5_{qui}), 59.17 ($2NCH_2$), 55.48 ($4NCH_{2pip}$), 53.64 ($4NCH_{2pip}$), 46.28 ($2NCH_3$), 41.08 ($2NCH_2$), 28.50 ($2NCH_2$), 25.22 ($2NCH_2$); ESI-MS m/z $[M+H]^+$ Calcd for $C_{43}H_{54}N_9O_2$: 728.440, Found: 728.465.

2,2'-(Pyridine-2,6-diyl)bis(N-(2-morpholinoethyl)quinoline-4-carboxamide) (1g)

Yellow crystals (yield, 68%), mp = 165-167 °C; ^{1}H NMR δ (300 MHz, $CDCl_3$ and 10% MeOD) 8.84 (s, 2H, -CH), 8.72 (d, 2H, J = 7.80 Hz, -CH), 8.32 (d, 2H, J= 8.20 Hz, -CH), 8.25 (d, 2H, J= 8.20 Hz, -CH), 8.10 (t, 1H, J = 7.80 Hz, -CH), 7.80 (t, 2H, J= 8.20 Hz, -CH), 7.64 (t, 2H, J= 8.20 Hz, -CH), 3.74 (t, 4H, J = 6.10 Hz, $-CH_2$), 3.69 (t, 8H, J = 4.70 Hz, OCH_2), 2.74 (t, 4H, J = 6.10 Hz, NCH_2), 2.61-2.58 (m, 8H, $-CH_{2morph}$) ; ^{13}C NMR δ (100 MHz, $CDCl_3$) 169.37 (2C=O), 157.09 (C-2_{pyr} and C-6_{pyr}), 156.52 (2C-2_{qui}), 149.76 (2C-$8a_{qui}$), 144.64 (2C-4_{qui}), 139.58 (C-4_{pyr}), 131.57 (2C-6_{qui} and 2C-8_{qui}), 129.25 (2C-7_{qui}), 126.53 (2C-3_{qui}), 125.90 (2C-$4a_{qui}$), 123.87 (C-3_{pyr} and C-5_{pyr}), 118.35 (2C-5_{qui}), 68.03 ($4OCH_2$), 58.55 ($2NCH_2$), 53.72 ($4NCH_{2pip}$), 54.73 ($4NCH_{2morph}$), 37.60 ($2NCH_2$); ESI-MS m/z $[M+H]^+$ Calcd for $C_{37}H_{40}N_7O_4$: 646.314, Found: 646.357.

2,2'-(Pyridine-2,6-diyl)bis(N-(2-(piperidin-1-yl)ethyl) quinoline-4-carboxamide) (1i)

Beige crystals (yield, 64%), mp = 174-176 °C; ^{1}H NMR δ (300 MHz, $CDCl_3$ and 10% MeOD) 8.82 (s, 2H, -CH), 8.70 (d, 2H, J = 7.80

Hz, -CH), 8.30 (d, 2H, J= 8.10 Hz, -CH), 8.24 (d, 2H, J= 8.10 Hz, -CH), 8.15 (t, 1H, J = 7.80 Hz, -CH), 7.82 (t, 2H, J = 7.80 Hz, -CH), 7.66 (t, 2H, J = 7.80 Hz, -CH), 3.72 (t, 4H, J = 6.60 Hz, -CH_2), 2.74 (t, 4H, J = 6.60 Hz, -CH_2), 2.60-2.54 (m, 8H, -NCH_{2pip}), 1.64-1.58 (m, 8H, -CH_{2pip}), 1.50-1.46 (m, 4H, -CH_{2pip}); ^{13}C NMR δ (100 MHz, $CDCl_3$) 169.94 (2C=O), 157.09 (C-2_{pyr} and C-6_{pyr}), 156.55 (2C-2_{qui}), 149.62 (2C-$8a_{qui}$), 144.45 (2C-4_{qui}), 139.60 (C-4_{pyr}), 131.63 (2C-6_{qui}), 131.12 (2C-8_{qui}), 129.24 (2C-7_{qui}), 126.60 (2C-3_{qui}), 125.91 (2C-$4a_{qui}$), 123.85 (C-3_{pyr} and C-5_{pyr}), 118.32 (2C-5_{qui}), 58.92 ($2NCH_2$), 55.75 ($4NCH_{2pip}$), 38.13 ($2NCH_3$), 26.77 ($4CH_{2pip}$), 25.22 ($2CH_{2pip}$); ESI-MS m/z $[M+H]^+$ Calcd for $C_{39}H_{44}N_7O_2$: 674.345, Found: 674.361.

2,2'-(Pyridine-2,6-diyl)bis(N-(2-(pyrrolidin-1-yl)ethyl) quinoline-4-carboxamide) (1k)

Beige crystals (yield, 70%), mp = 179-181 °C; ^{1}H NMR d (300 MHz, $CDCl_3$ and 10% MeOD) 8.83 (s, 2H, -CH), 8.70 (d, 2H, J = 7.80 Hz, -CH), 8.29 (d, 2H, J= 8.40 Hz, -CH), 8.24 (d, 2H, J= 8.40 Hz, -CH), 8.14 (t, 1H, J = 7.80 Hz, -CH), 7.82 (t, 2H, J = 7.80 Hz, -CH), 7.66 (t, 2H, J = 7.80 Hz, -CH), 3.72 (t, 4H, J = 6.60 Hz, -CH_2), 2.87 (t, 4H, J = 6.60 Hz, -CH_2), 2.71-2.67 (m, 8H, -NCH_{2pyr}), 1.85-1.82 (m, 8H, -CH_{2pyr}); ^{13}C NMR δ (100 MHz, $CDCl_3$) 165.86 (2C=O), 152.87 (C-2_{pyr} and C-6_{pyr}), 152.35 (2C-2_{qui}), 145.42 (2C-$8a_{qui}$), 139.84 (2C-4_{qui}), 135.41 (C-4_{pyr}), 127.43 (2C-6_{qui}), 126.93 (2C-8_{qui}), 125.05 (2C-7_{qui}), 122.36 (2C-3_{qui}), 121.70 (2C-$4a_{qui}$), 119.66 (C-3_{pyr} and C-5_{pyr}), 114.20 (2C-5_{qui}), 51.97 ($2NCH_2$), 51.21 ($4NCH_{2pyr}$), 35.62 ($2NCH_2$), 20.34 ($4CH_{2pyr}$); ESI-MS m/z $[M+H]^+$ Calcd for $C_{37}H_{40}N_7O_2$: 646.314, Found: 646.322.

2,2'-(Pyridine-2,6-diyl)bis(N-(3-(1H-imidazol-1-yl)propyl) quinoline-4-carboxamide) (1n)

Beige crystals (yield, 68%), mp = 185-187 °C; ^{1}H NMR δ (300 MHz, $CDCl_3$ and 10% MeOD) 8.79 (s, 2H, -CH), 8.68 (d, 2H, J = 7.80 Hz, -CH), 8.24 (d, 4H, J= 8.40 Hz, -CH), 8.14 (t, 1H, J = 7.80 Hz, -CH), 7.81 (t, 2H, J = 7.80 Hz, -CH), 7.65 (t, 2H, J = 7.80 Hz, -CH), 7.58 (s, 2H, -$CH_{imidazol}$), 7.06 (s, 2H, -$CH_{imidazol}$), 6.97 (s, 2H, -$CH_{imidazol}$), 4.14 (t, 4H, J = 6.90 Hz, -CH_2), 3.48 (t, 4H, J = 6.90 Hz, -CH_2), 2.18 (qt, 4H, J = 6.90 Hz, -CH_2); ESI-MS m/z $[M+H]^+$ Calcd for $C_{37}H_{37}N_9O_2$: 636.283, Found: 636.325.

2,2'-(Pyridine-2,6-diyl)bis(N-(2-(dimethylamino)ethyl) quinoline-6-carboxamide) (2a)

Yellow-orange crystals (yield, 59%), mp = 166-168 °C; ^{1}H NMR δ (300 MHz, $CDCl_3$ and 10% MeOD) 8.78 (d, 2H, J = 8.70 Hz, -CH), 8.66 (d, 2H, J= 8.10 Hz, -CH), 8.39-8.36 (m, 4H, -CH), 8.18-8.08 (m, 4H, -CH), 8.03 (t, 1H, J = 7.80 Hz, -CH), 3.53 (t, 4H, J = 5.70 Hz, -NCH_2), 2.54 (t, 4H, J = 5.70 Hz, -NCH_2), 2.27 (s, 12H, -$N(CH_3)_2$); ESI-MS m/z $[M+H]^+$ Calcd for $C_{33}H_{36}N_7O_2$: 562.293, Found: 562.530.

2,2'-(Pyridine-2,6-diyl)bis(N-(3-(dimethylamino)propyl) quinoline-6-carboxamide) (2b)

Beige crystals (yield, 62%), mp = 168-170 °C; ^{1}H NMR δ (300 MHz, $CDCl_3$ and 10% MeOD) 8.86 (d, 2H, J = 8.70 Hz, -CH), 8.73 (d, 2H, J= 7.80 Hz, -CH), 8.42-8.40 (m, 2H, -CH), 8.24 (d, 2H, J = 8.70 Hz, -CH), 8.16-8.11 (m, 3H, -CH), 3.51 (t, 4H, J = 6.90 Hz, -NCH_2), 2.46 (t, 4H, J = 6.90 Hz, -NCH_2), 2.30 (s, 12H, -$N(CH_3)_2$), 1.84 (qt, 4H, J = 6.90 Hz, -NCH_2); ^{13}C NMR δ (100 MHz, $CDCl_3$) 168.85 (2C=O), 158.80 (C-2_{pyr} and C-6_{pyr}), 156.40 (2C-2_{qui}), 150.16 (2C-$8a_{qui}$), 139.44 (C-4_{pyr}), 139.27 (2C-4_{qui}), 133.78 (2C-6_{qui}), 130.98 (2C-5_{qui}), 128.83 (2C-8_{qui} and 2C-7_{qui}), 123.88 (C-3_{pyr} and C-5_{pyr}), 121.22 (2C-3_{qui}), 118.87 (2C-$4a_{qui}$), 58.71 ($2NCH_2$), 46.29 ($2N(CH_3)_2$), 40.13 ($2NCH_2$), 27.57 ($2CH_2$); ESI-MS m/z $[M+H]^+$ Calcd $C_{35}H_{40}N_7O_2$: 590.324, Found: 590.333.

2,2'-(Pyridine-2,6-diyl)bis(N-(3-(4-methylpiperazin-1-yl) propyl)quinoline-6-carboxamide) (2c)

Orange crystals (yield, 71%), mp = 175-177 °C; ^{1}H NMR δ (300 MHz, $CDCl_3$ and 10% MeOD) 8.92 (d, 2H, J = 8.70 Hz, -CH), 8.82 (d, 2H, J= 7.80 Hz, -CH), 8.75 (bs, 2H, -NH), 8.48-8.42 (m, 4H, -CH), 8.28-8.17 (m, 4H, -CH), 8.12 (t, 1H, J = 7.80 Hz, -CH), 3.69 (q, 4H, J = 6.20 Hz, -NCH_2), 2.67 (t, 4H, J = 6.20 Hz, -NCH_2), 2.63-2.42 (m, 16H, -CH_{2pip}), 2.32 (s, 6H, -NCH_3), 1.94-1.81 (m, 4H, -CH_2); ESI-MS m/z $[M+H]^+$ Calcd for Calcd for $C_{41}H_{50}N_9O_2$: 700.409, Found: 700.391.

2,2'-(Pyridine-2,6-diyl)bis(N-(3-(piperidin-1-yl)propyl) quinoline-6-carboxamide) (2d)

Beige crystals (yield, 69%), mp = 166-168 °C; ^{1}H NMR δ (300 MHz, $CDCl_3$ and 10% MeOD) 9.15 (t, 2H, J = 5.40 Hz, -NH), 8.92 (d, 2H, J = 8.70 Hz, -CH), 8.81 (d, 2H, J= 7.80 Hz, -CH), 8.46-8.44 (m, 2H, -CH), 8.41 (d, 2H, J = 8.70 Hz, -CH), 8.28-8.18 (m, 4H, -CH), 8.12 (t, 1H, J = 7.80 Hz, -CH), 3.67 (q, 4H, J = 5.40 Hz, -NCH_2), 2.61 (t, 4H, J = 5.40 Hz, -NCH_2), 2.52-2.46 (m, 8H, -NCH_{2pip}), 1.66-1.61 (m, 8H, -CH_{2pip}), 1.54-1.51 (m, 4H, -CH_{2pip}); ESI-MS m/z $[M+H]^+$ Calcd for $C_{41}H_{48}N_7O_2$: 670.387, Found: 670.395.

2,2'-(Pyridine-2,6-diyl)bis(N-(3-(pyrrolidin-1-yl)propyl) quinoline-6-carboxamide) (2e)

Beige crystals (yield, 53%), mp = 171-173 °C; ^{1}H NMR δ (300 MHz, $CDCl_3$ and 10% MeOD) 9.31 (t, 2H, J = 5.70 Hz, -NH), 8.91 (d, 2H, J = 8.70 Hz, -CH), 8.81 (d, 2H, J= 7.80 Hz, -CH), 8.39 (d, 2H, J = 8.70 Hz, -CH), 8.38-8.37 (m, 2H, -CH), 8.24 (d, 2H, J = 8.70 Hz, -CH), 8.14-8.09 (m, 2H, -CH), 8.11 (t, 1H, J = 7.80 Hz, -CH), 3.69 (q, 4H, J = 5.70 Hz, $-NCH_2$), 2.81 (t, 4H, J = 5.70 Hz, $-NCH_2$), 2.67-2.64 (m, 8H, $-NCH_{2pip}$), 1.92-1.72 (m, 12H, $-CH_{2pip}$); ^{13}C NMR δ (100 MHz, $CDCl_3$) 172.77 (2C=O), 162.86 (C-2_{pyr} and C-6_{pyr}), 160.45 (2C-2_{qui}), 154.27 (2C-$8a_{qui}$), 143.47 (C-4_{pyr}), 143.24 (2C-4_{qui}), 137.60 (2C-6_{qui}), 135.08 (2C-5_{qui}), 132.87 (2C-8_{qui} and 2C-7_{qui}), 127.91 (C-3_{pyr} and C-5_{pyr}), 125.25 (2C-3_{qui}), 118.84 (2C-$4a_{qui}$), 59.24 ($2NCH_{2pyr}$), 43.98 ($2NCH_2$), 31.73 ($2NCH_2$), 28.56 ($2CH_2$ and $2CH_{2pyr}$); ESI-MS m/z $[M+H]^+$ Calcd $C_{39}H_{44}N_7O_2$: 642.355, Found: 642.367.

2,2'-(Pyridine-2,6-diyl)bis(N-(3-((3-(dimethylamino)propyl) amino)propyl)quinoline-6-carboxamide) (2f)

Orange crystals (yield, 50%), mp = 235-237 °C; ^{1}H NMR δ (300 MHz, $CDCl_3$ and 10% MeOD) 8.89 (d, 2H, J = 8.70 Hz, -CH), 8.80 (d, 2H, J= 7.80 Hz, -CH), 8.73 (t, 2H, J = 5.40 Hz, -NH), 8.45-8.43 (m, 2H, -CH), 8.42 (d, 2H, J = 8.70 Hz, -CH), 8.23 (d, 2H, J = 8.70 Hz, -CH), 8.17-8.10 (m, 2H, -CH), 8.13 (t, 1H, J = 7.80 Hz, -CH), 3.69 (q, 4H, J = 5.70 Hz, $-NCH_2$), 2.93 (t, 4H, J = 5.70 Hz, $-NCH_2$), 2.77 (t, 4H, J = 6.90 Hz, $-NCH_2$), 2.38 (t, 4H, J = 6.90 Hz, $-NCH_2$), 2.21 (s, 12H, $-N(CH_3)_2$), 1.93-1.71 (m, 8H, $-CH_2$); ^{13}C NMR δ (100 MHz, $CDCl_3$) 166.60 (2C=O), 157.35 (C-2_{pyr} and C-6_{pyr}), 155.21 (2C-2_{qui}), 149.04 (2C-$8a_{qui}$), 149.00 (C-4_{pyr}), 138.06 (2C-4_{qui}), 137.64 (2C-6_{qui}), 132.91 (2C-5_{qui}), 130.01 (2C-8_{qui}), 127.68 (2C-7_{qui}), 127.43 (C-3_{pyr} and C-5_{pyr}), 122.51 (2C-3_{qui}), 119.71 (2C-$4a_{qui}$), 58.08 ($2NCH_2$), 49.35 ($2NCH_2$), 48.66 ($2NCH_2$), 45.54 ($2N(CH_3)_2$), 40.65 ($2NCH_2$), 27.83 ($4CH_2$); ESI-MS m/z $[M+H]^+$ $C_{41}H_{54}N_9O_2$: 704.440, Found: 704.451.

2,2'-(Pyridine-2,6-diyl)bis(N-(3-(1H-imidazol-1-yl)propyl) quinoline-6-carboxamide) (2g)

Beige crystals (yield, 71%), mp = 188-190 °C; ^{1}H NMR δ (300 MHz, $CDCl_3$ and 10% MeOD) 8.84 (d, 2H, J = 8.70 Hz, -CH), 8.71 (d, 2H, J= 7.80 Hz, -CH), 8.45 (d, 2H, J = 8.70 Hz, -CH), 8.39-8.37 (m, 2H, -CH), 8.21 (d, 2H, J = 8.70 Hz, -CH), 8.12 (d, 2H, J = 8.70 Hz, -CH), 8.11 (t, 1H, J = 7.80 Hz, -CH), 7.60 (s, 2H, $-CH_{imidazol}$), 7.05 (s, 2H, $-CH_{imidazol}$), 6.99 (s, 2H, $-CH_{imidazol}$), 4.10 (t, 4H, J = 6.90 Hz, $-NCH_2$), 3.48 (t, 4H, J = 6.90 Hz, $-NCH_2$), 2.16 (qt, 4H, J = 6.90 Hz, $-CH_2$); ^{13}C NMR δ (100 MHz, $CDCl_3$) 169.47 (2C=O), 158.99 (C-2_{pyr} and C-6_{pyr}), 156.51 (2C-2_{qui}), 150.30 (2C-$8a_{qui}$), 139.57 ($CH_{imidazol}$), 139.38 (C-4_{pyr}), 138.31 (2C-4_{qui}), 133.63 (2C-6_{qui}), 131.07 (2C-5_{qui}), 129.91 (2C-8_{qui}), 129.07 (2C-7_{qui}), 124.02 (C-3_{pyr} and C-5_{pyr}), 121.36 ($2CH_{imidazol}$), 120.55 (2C-3_{qui}), 118.78 (2C-$4a_{qui}$), 46.18 ($2NCH_2$), 38.61 ($2NCH_2$), 32.21 ($2CH_2$); ESI-MS m/z $[M+H]^+$ Calcd for $C_{37}H_{37}N_9O_2$: 636.283, Found: 636.753.

2,2'-(Pyridine-2,6-diyl)bis(N-(3-(dimethylamino)propyl) quinoline-7-carboxamide) (3a)

Yellow crystals (yield, 69%), mp = 158-160 °C; ^{1}H NMR δ (300 MHz, $CDCl_3$ and 10% MeOD) 8.74 (d, 2H, J = 8.70 Hz, -CH), 8.58 (d, 2H, J= 7.80 Hz, -CH), 8.44 (s, 2H, -CH), 8.29 (d, 2H, J = 8.40 Hz, -CH), 8.01 (t, 1H, J = 7.80 Hz, -CH), 7.91 (d, 2H, J = 8.40 Hz, -CH), 7.85 (d, 2H, J = 8.40 Hz, -CH), 3.40 (t, 4H, J = 6.90 Hz, $-NCH_2$), 2.35 (t, 4H, J = 6.90 Hz, $-NCH_2$), 2.19 (s, 12H, $-N(CH_3)_2$), 1.73 (qt, 4H, J = 6.90 Hz, $-NCH_2$); ^{13}C NMR δ (100 MHz, $CDCl_3$) 167.59 (2C=O), 156.79 (C-2_{pyr} and C-6_{pyr}), 155.02 (2C-2_{qui}), 146.94 (2C-$8a_{qui}$), 137.99 (C-4_{pyr}), 136.67 (2C-4_{qui}), 135.43 (2C-7_{qui}), 129.65 (2C-$4a_{qui}$), 127.95 (2C-5_{qui} and 2C-8_{qui}), 125.08 (2C-6_{qui}), 122.14 (2C-3_{qui}), 120.37 (C-3_{pyr} and C-5_{pyr}), 57.23 ($2NCH_2$), 44.78 ($2N(CH_3)_2$), 38.62 ($2NCH_2$), 26.18 ($2CH_2$); ESI-MS m/z $[M+H]^+$ Calcd $C_{35}H_{40}N_7O_2$: 590.324, Found: 590.387.

2,2'-(Pyridine-2,6-diyl)bis(N-(3-(4-methylpiperazin-1-yl) propyl)quinoline-7-carboxamide) (3b)

Beige crystals (yield, 65%), mp = 161-163 °C; ^{1}H NMR δ (300 MHz, $CDCl_3$ and 10% MeOD) 8.88 (d, 2H, J = 8.40 Hz, -CH), 8.75 (d, 2H, J= 8.10 Hz, -CH), 8.57 (s, 2H, -CH), 8.38 (d, 2H, J = 8.40 Hz, -CH), 8.11-8.05 (m, 3H, -CH), 7.96 (d, 2H, J = 8.70 Hz, -CH), 3.61 (t, 4H, J = 5.70 Hz, $-NCH_2$), 2.61 (t, 4H, J = 5.70 Hz, $-NCH_2$), 2.60-2.45 (m, 16H, $-CH_{2pip}$), 2.17 (s, 6H, $-NCH_3$), 1.86 (qt, 4H, J = 5.70 Hz, $-CH_2$); ^{13}C NMR δ (100 MHz, $CDCl_3$) 168.65 (2C=O), 158.16 (C-2_{pyr} and C-6_{pyr}), 156.54 (2C-2_{qui}), 148.55 (2C-$8a_{qui}$), 139.21 (C-4_{pyr}), 138.05 (2C-4_{qui}), 137.17 (2C-7_{qui}), 131.21 (2C-$4a_{qui}$), 129.53 (2C-5_{qui}), 129.46 (2C-8_{qui}), 126.98 (2C-6_{qui}), 123.66 (2C-3_{qui}), 121.71 (C-3_{pyr} and C-5_{pyr}), 59.15 ($2NCH_2$), 56.15 ($4NCH_{2pip}$), 54.35 ($4NCH_{2pip}$), 47.05 ($2NCH_3$), 41.85 ($2NCH_2$), 25.75 ($2CH_2$); ESI-MS m/z $[M+H]^+$ Calcd for Calcd for $C_{41}H_{50}N_9O_2$: 700.409, Found: 700.436.

2,2'-(Pyridine-2,6-diyl)bis(N-(3-(piperidin-1-yl)propyl) quinoline-7-carboxamide) (3c)

Beige crystals (yield, 57%), mp = 148-150 °C; ^{1}H NMR δ (300 MHz, $CDCl_3$ and 10% MeOD) 8.89 (d, 2H, J = 8.40 Hz, -CH), 8.72

(d, 2H, J= 7.80 Hz, -CH), 8.63 (s, 2H, -CH), 8.45 (d, 2H, J = 8.70 Hz, -CH), 8.14 (t, 1H, J = 7.80 Hz, -CH), 8.06-8.00 (m, 4H, -CH), 3.54 (t, 4H, J = 6.60 Hz, $-NCH_2$), 2.52 (t, 4H, J = 6.60 Hz, $-NCH_2$), 2.50-2.46 (m, 8H, $-NCH_{2pip}$), 1.89 (qt, 4H, J = 6.60 Hz, $-CH_2$), 1.69-1.62 (m, 8H, $-CH_{2pip}$), 1.53-1.48 (m, 4H, $-CH_{2pip}$); ^{13}C NMR δ (100 MHz, $CDCl_3$) 167.67 (2C=O), 156.58 (C-2_{pyr} and C-6_{pyr}), 154.86 (2C-2_{qui}), 146.73 (2C-$8a_{qui}$), 137.69 (C-4_{pyr}), 136.45 (2C-4_{qui}), 135.12 (2C-7_{qui}), 129.52 (2C-$4a_{qui}$), 127.89 (2C-5_{qui}), 127.75 (2C-8_{qui}), 124.76 (2C-6_{qui}), 121.85 (2C-3_{qui}), 120.11 (C-3_{pyr} and C-5_{pyr}), 56.93 ($2NCH_2$), 53.99 ($4NCH_{2pip}$), 38.85 ($2NCH_2$), 24.93 ($4CH_{2pip}$), 24.75 ($2CH_2$), 23.52 ($2CH_2$); ESI-MS m/z $[M+H]^+$ Calcd for $C_{41}H_{48}N_7O_2$: 670.387, Found: 670.559.

2,2'-(Pyridine-2,6-diyl)bis(N-(3-(pyrrolidin-1-yl)propyl) quinoline-7-carboxamide) (3d)

Beige crystals (yield, 67%), mp = 144-146 °C; ^1H NMR δ (300 MHz, $CDCl_3$ and 10% MeOD) 8.86 (d, 2H, J = 8.70 Hz, -CH), 8.70 (d, 2H, J= 7.80 Hz, -CH), 8.55 (s, 2H, -CH), 8.40 (d, 2H, J = 8.40 Hz, -CH), 8.11 (t, 1H, J = 7.80 Hz, -CH), 8.05-8.01 (m, 2H, -CH), 7.96 (d, 2H, J = 8.40 Hz, -CH), 3.56 (t, 4H, J = 6.30 Hz, $-NCH_2$), 2.68 (t, 4H, J = 6.30 Hz, $-NCH_2$), 2.68-2.62 (m, 8H, $-NCH_{2pyr}$), 1.91-1.87 (m, 12H, $-CH_2$ and $-CH_{2pip}$); ESI-MS m/z $[M+H]^+$ Calcd $C_{39}H_{44}N_7O_2$: 642.355, Found: 642.558.

2,2'-(Pyridine-2,6-diyl)bis(N-(3-(1H-imidazol-1-yl)propyl) quinoline-7-carboxamide) (3e)

Beige crystals (yield, 60%), mp = 173-175 °C; ^1H NMR δ (300 MHz, $CDCl_3$ and 10% MeOD) 8.99-8.91 (m, 4H, -CH), 8.70 (d, 2H, J= 7.80 Hz, -CH), 8.69 (s, 2H, -CH), 8.31 (t, 1H, J = 7.80 Hz, -CH), 8.18 (d, 2H, J = 8.10 Hz, -CH), 8.08 (d, 2H, J = 7.80 Hz, -CH), 7.71 (s, 2H, $-CH_{imidazol}$), 7.26 (s, 2H, $-CH_{imidazol}$), 6.92 (s, 2H, $-CH_{imidazol}$), 4.09 (t, 4H, J = 6.60 Hz, $-NCH_2$), 3.35 (t, 4H, J = 6.60 Hz, $-NCH_2$), 2.04 (qt, 4H, J = 6.60 Hz, $-CH_2$); ESI-MS m/z $[M+H]^+$ Calcd for $C_{37}H_{37}N_9O_2$: 636.283, Found: 636.299.

General procedure for the synthesis of 2,2'-(pyridine-2,6-diyl) bis(quinoline-6-carboxylic acid) (6) and 2,2'-(pyridine-2,6-diyl)bis(quinoline-7-carboxylic acid) (8)

To a suspension of methyl 4-amino-2-formylbenzoate or methyl 3-amino-4-formylbenzoate (1.6 mmol) in 15 mL of NaOH (33%) aqueous solution was added 2,6-diacetyl pyridine (0.8 mmol). The reaction mixture was then refluxed under stirring for 2 h. The reaction mixture was cooled and the precipitate was filtered, washed with minimum amount of cold water and then with diethyl ether (2 times). After drying the precipitate was dissolved in hot 10 mL water and 6N HCl was used to adjust the pH to 5. The dark precipitate was filtered and washed with water and then petroleum ether for drying to get product 6 or 8.

2,2'-(Pyridine-2,6-diyl)bis(quinoline-6-carboxylic acid) (6)

Dark-red crystals (yield, 48%), mp > 260 °C; ESI-MS m/z $[M+H]^+$ Calcd for $C_{25}H_{16}N_3O_4$: 422.114, Found: 422.161.

2,2'-(Pyridine-2,6-diyl)bis(quinoline-7-carboxylic acid) (8)

Dark-red crystals (yield, 51%), mp > 260 °C; ESI-MS m/z $[M+H]^+$ Calcd for $C_{25}H_{16}N_3O_4$: 422.114, Found: 422.142.

General procedure for 2,2'-(pyridine-2,6-diyl)bis(N-((substituted-amino)alkyl)quinoline-carboxamide) 1-3 oxalates salts -m (COOH)2

To a solution of compounds **1-3** (0.15 mmol) in a mixture of isopropanol (7 mL)/dichloromethane (4 mL)/methanol (1 mL) was added oxalic acid (0.9 mmol, 6 eq.). The reaction mixture was heated under reflux for 20 minutes. The precipitate was filtered, washed with isopropanol then with diethyl ether and dried under reduced pressure to give the oxalate salts of 1-3.

Biology

In vitro antiplasmodial activity

Derivatives 1-3 were dissolved in DMSO then diluted in sterile water in order to obtain a range of concentration from 40 nM to 40 mM for a first screening against culture-adapted *Plasmodium falciparum* reference strains 3D7 and W2. The former strain is susceptible to chloroquine (CQ) but displays a decreased susceptibility to mefloquine (MQ); the latter is considered resistant to CQ. These two strains are obtained from the collection of the National Museum of Natural History (Paris, France). The parasites were cultivated in RPMI medium (Sigma-Aldrich, Lyon, France) supplemented with 0.5% Albumax I (Life Technologies Corporation, Paisley, UK), hypoxanthine (Sigma-Aldrich), and gentamicin (Sigma-Aldrich) with human erythrocytes and were

incubated at 37 °C in a candle jar, as described previously [28]. The *P. falciparum* drug susceptibility test was carried out in 96-well flat bottom sterile plates in a final volume of 250 µL. After 48 h incubation period with the drugs, quantities of DNA in treated and control cultures of parasites in human erythrocytes were quantified using the SYBR Green I (Sigma-Aldrich) fluorescence-based method [29,30]. Briefly, after incubation, plates were frozen at -20 °C until use. Plates were then thawed for 2 h at room temperature, and 100 µL of each homogenized culture was transferred to a well of a 96-well flat bottom sterile black plate (Nunc, Inc.) that contained 100 µL of the SYBR Green I lysis buffer (2xSYBR Green, 20 mM Tris base pH 7.5, 5 mM EDTA, 0.008% w/v saponin, 0.08% w/v Triton X-100). Negative controls treated with solvent (typically DMSO or H_2O), and positive controls (CQ and MQ) were added to each set of experiments. Plates were incubated for 1 h at room temperature and then read on a fluorescence plate reader (Tecan, Austria) using excitation and emission wavelengths of 485 and 535 nm, respectively. The concentrations at which the screening drug or antimalarial is capable of inhibiting 50% of parasitic growth (IC_{50}) are calculated from a sigmoid inhibition model Emax with an estimate of IC_{50} by non-linear regression (IC Estimator version 1.2) and are reported as means calculated from three independent experiments [31].

In vitro antileishmanial activity

L. donovani (MHOM/IN/00/DEVI) used in this study was provided by the CNR Leishmania (Montpellier, France). The effects of the tested compounds on the growth of *L. donovani* (MHOM/IN/00/DEVI) promastigotes were assessed by MTT assay [32]. Briefly, promastigotes in log-phase in Schneider's medium supplemented with 20% fetal calf serum (FCS), 2 mM L-glutamine and antibiotics (100 U/mL penicillin and 100 µg/mL streptomycin), were incubated at an average density of 10^6 parasites/mL in sterile 96-well plates with various concentrations of compounds previously dissolved in DMSO (final concentration less than 0.5% v/v), in duplicate. Appropriate controls treated with DMSO, pentamidine and amphotericin B (reference drugs purchased from Sigma-Aldrich) were added to each set of experiments. Duplicate assays were performed for each sample. After 72 h incubation period at 27 °C, parasite metabolic activity was determined. Each well was microscopically examined for precipitate formation. To each well was added 10 µL of 10 mg/mL MTT [3-(4,5-dimethylthiazol-2-yl)-2,5-diphenyltetrazolium bromide)] solution followed by 4 h incubation time. The enzyme reaction was stopped by addition of 100 µL of 50% isopropanol/10% sodium dodecyl sulfate [33]. Plates were vigorously shaken (300 rpm) for 10 min, and the absorbance was measured at 570 nm with 630 nm as reference wavelength in a BIOTEK ELx808 Absorbance Microplate Reader (Agilent Technologies, Les Ulis, France). The IC_{50} was defined as the concentration of drug required to inhibit by 50% of the metabolic activity of *L. donovani* promastigotes compared to the control. IC_{50} of the parasite's growth (half maximal inhibitory concentration or IC_{50} values) were then calculated from the obtained experimental results using a previously described regression program [31]. IC_{50} values were calculated from three independent experiments.

In vitro antitrypanosomal activity

The effects of the tested compounds on the growth of *T. brucei brucei* were assessed using an Alamar Blue® assay described by Räz., *et al*. [34] *T. brucei brucei* AnTat 1.9 (IMTA, Antwerpen, Belgium) was cultured in MEM with Earle's salts, supplemented according to the protocol of Baltz., *et al*. [35] with the following modifications: 0.5 mM mercaptoethanol (Sigma Aldrich), 1.5 mM L-cysteine (Sigma Aldrich), 0.05 mM bathocuproine sulfate (Sigma Aldrich), and 20% heat-inactivated horse serum (Gibco, France) at 37 °C and 5% CO_2. Samples were incubated at an average density of 2000 parasites/well in sterile 96-wells plates (Fisher, France) with various concentrations of compounds dissolved in DMSO. All doses were tested in duplicate. Appropriate controls treated with solvents 0.9% NaCl or DMSO or with suramin, pentamidine, eflornithine, and fexinidazole (reference drugs purchased from Sigma Aldrich and Fluorochem, UK) were added to each set of experiments. After 69 h incubation period at 37 °C, 10 µL of the viability marker Alamar Blue (Fisher) was added to each well, and the plates were incubated for 5 h. The plates were read in a PerkinElmer ENSPIRE (Germany) microplate reader using an excitation wavelength of 530 nm and an emission wavelength of 590 nm. The IC_{50} was defined as the concentration of drug necessary to inhibit by 50% the activity of *T. brucei brucei* compared to the control. IC_{50} values were calculated using a nonlinear regression analysis of dose-response curves performed using GraphPad Prism software (GraphPad Software, San Diego, CA, USA). IC_{50} values were calculated from three independent experiments.

Cytotoxicity evaluation

A cytotoxicity evaluation was performed using the method reported by Mosmann [32] with slight modifications to determine the cytotoxic concentrations 50% (CC_{50}) and using doxorubicin as a cytotoxic reference compound. These assays were performed in human HepG2 cells purchased from ATCC (ref HB-8065). These cells are a commonly used human hepatocarcinoma-derived cell line that has characteris-tics similar to those of primary hepatocytes. These cells express many hepatocyte-specific metabolic enzymes, thus enabling the cytotoxicity of tested product metabolites to be evaluated. Briefly, cells in 100 µL of complete RPMI medium, [RPMI supplemented with 10% FCS, 1% L-glutamine (200 mM), penicillin (100 U/mL), and streptomycin (100 µg/mL)] were inoculated at 37 °C into each well of 96-well plates in a humidified chamber in 6% CO_2. After 24 h, 100 µL of medium with test compound at various concentrations dissolved in DMSO (final concentration less than 0.5% v/v) were added, and the plates were incubated for 72 h at 37 °C. Duplicate assays were performed for each sample. Each well was microscopically examined for precipitate formation before the medium was aspirated from the wells. After aspiration, 100 µL of MTT solution (0.5 mg/mL in medium without FCS) were then added to each well. Cells were incubated for 2 h at 37 °C. The MTT solution was removed, and DMSO (100 µL) was added to dissolve the resulting blue formazan crystals. Plates were shaken vigorously (300 rpm) for 5 min. The absorbance was measured at 570 nm with 630 nm as reference wavelength in a BIO-TEK ELx808 Absorbance Microplate Reader. DMSO was used as blank and doxorubicin (Sigma Aldrich) as positive con-trol. Cell viability was calculated as percentage of control (cells incubated without compound). The CC_{50} was determined from the dose-response curve using the Table-Curve 2D V5.0 software (Systat Software, Palo Alto, CA, USA).

FRET melting experiments

Some of our new antiprotozoal bioactive derivatives 1-3 have been selected for the subsequent FRET melting experiments. These were performed with dual-labeled oligonucleotides mimicking the Plasmodium telomeric sequences FPf1T [FAM-5'(GGGTTTA)3-GGG3'-TAMRA] and FPf8T [FAM-5'(GGGTTCA)3GGG3'-TAMRA], the Trypanosoma 9 and 11 chromosomic sequence FTrypBT (also named FEBR1T) [FAM-5'GGGCAGGGGGTGATGGGGAGGAGCCAGGG3'-TAMRA], the human telomeric sequence F21T [FAM-(GGGTTA)3-GGG3'-TAMRA] and the human duplex sequence FdxT [FAM5'-TATAGCTATA-hexaethyleneglycol-TATAGCTATA3'-TAMRA] [16,18,20,36]. The oligonucleotides were pre-folded in 10 mM lithium cacodylate buffer (pH 7.2), with 10 mM KCl and 90 mM LiCl (K^+ condition). The FAM emissions were recorded at 516 nm using a 492 nm excitation wavelength in the absence and presence of a single compound as a function of temperature (25 to 95 °C) in 96-well microplates by using a Stratagene MX3000P real-time PCR device at a rate of 1 °C·min^{-1}. Data were normalized between 0 and 1, and the required temperature for half-denaturation of oligonucleotides corresponding to the emission value of 0.5 was taken as the Tm. Each experiment was performed in duplicate with 0.2 µM of labeled oligonucleotide and 5 µM of compound under K^+ condition. For each compound, three independent experiments were carried out.

Results and Discussion

Chemistry

The reported 2,6-di-(4-carbamoyl-2-quinolinyl)pyridine derivatives 1a-n were synthesized in three steps from the commercially available isatin and 2,6-diacetylpyridine (Scheme 1). 2,6-Diacetylpyridine reacts with isatin in alkaline condition through double Pfitzinger reaction to give the 2,2'-(pyridine-2,6-diyl)bis(quinoline-4-carboxylic acid) 4 after acidification with hydrochloric acid [37,38]. The diacid chloride 5 was obtained by refluxing the 2,6-di-(4-carboxy-2-quinolinyl)pyridine 4 in excess of thionyl chloride. This diacid chloride 5 was then coupled with various substituted aminoalkylamines to afford the 2,6-di-(4-carbamoyl-2-quinolinyl)pyridine derivatives 1a-n. These diquinolinylpyridine compounds 1a-n were then converted into their ammonium oxalate salts 1a-n by treatment with oxalic acid in refluxing isopropanol. Table 1 summarizes the physical properties of the new synthesized 1a-n oxalates. The structure of these new substituted derivatives 1 has been confirmed by ^1H and ^{13}C-NMR, and also ESI-MS analysis.

The same strategy was used for the synthesis of 2,6-di-(6-carbamoyl-2-quinolinyl)pyridine derivatives 2a-g (Series B) via the key intermediate di-acide 6, previously prepared through the coupling of 2,6-diacetylpyridine reacts with methyl 4-amino-2-

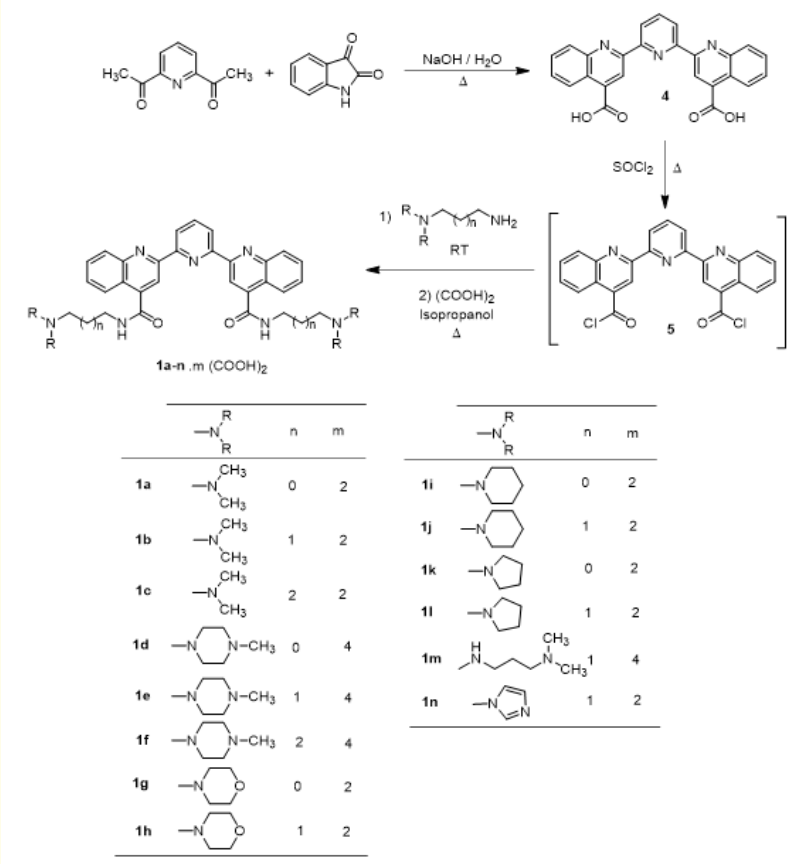

		n	m
1a	$-N(CH_3)_2$	0	2
1b	$-N(CH_3)_2$	1	2
1c	$-N(CH_3)_2$	2	2
1d	$-N\square N-CH_3$	0	4
1e	$-N\square N-CH_3$	1	4
1f	$-N\square N-CH_3$	2	4
1g	$-N\square O$	0	2
1h	$-N\square O$	1	2

		n	m
1i	$-N\square$	0	2
1j	$-N\square$	1	2
1k	$-N\square$	0	2
1l	$-N\square$	1	2
1m	$H-N-(CH_2)_1-N(CH_3)_2$	1	4
1n	$-N\square N$	1	2

Scheme 1: General procedure for the preparation of new 2,6-di-(4-carbamoyl-2-quinolinyl)pyridine derivatives 1a-n.

formylbenzoate in basic condition (Scheme 2) [39]. Reaction of thionyl chloride on this diacid 6 led to the intermediate diacid chloride 7 that was then submitted to different substituted aminoalkylamines to give the 2,6-di-(6-carbamoyl-2-quinolinyl) pyridine derivatives 2a-g. All compounds 2 were also converted into ammonium oxalate salts by treatment with oxalic acid in refluxing isopropanol.

The 2,6-di-(7-carbamoyl-2-quinolinyl)pyridine derivatives 3a-e (Series C) were synthesized via the di-acide 8. In this case, this diacid 8 was prepared through a reaction between 2,6-diacetylpyridine and methyl 3-amino-4-formylbenzoate in alkaline medium (Scheme 3). The action of thionyl chloride on 8 gave the intermediate diacid chloride 9. Reaction of various substituted aminoalkylamines on this diacid chloride 9 gave the 2,6-di-(7-carbamoyl-2-quinolinyl) pyridine derivatives 3a-e.

Biological evaluation

In vitro antimalarial activity

All these novel diquinolinyl-pyridine derivatives 1-3 were evaluated for their potential antimalarial activity *in vitro* by

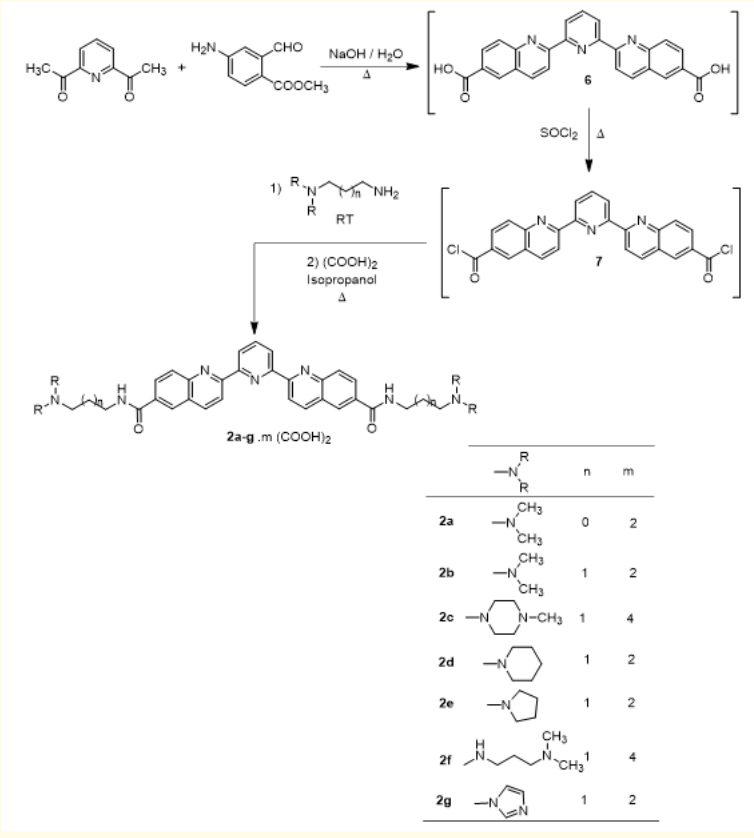

Scheme 2: General procedure for the preparation of new 2,6-di-(6-carbamoyl-2-quinolinyl)pyridine derivatives 2a-g.

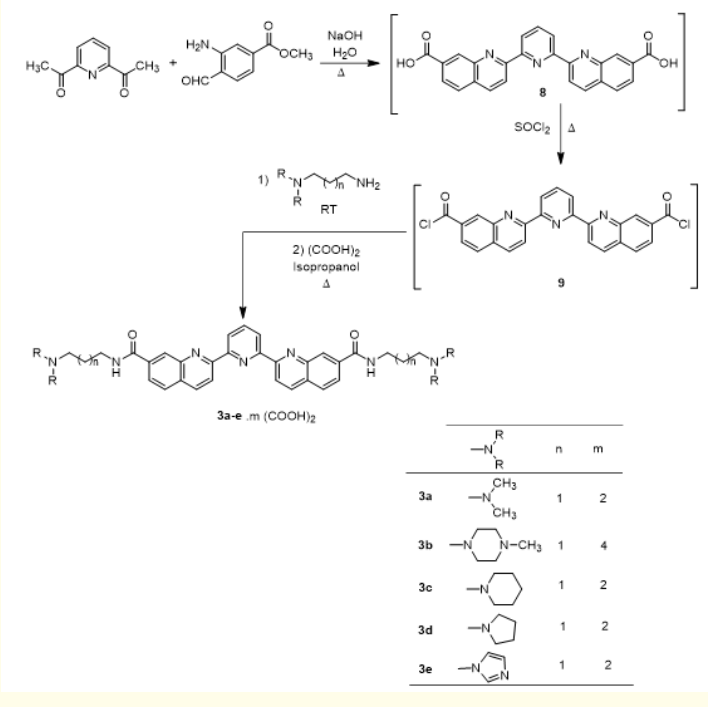

Scheme 3: General procedure for the preparation of new 2,6-di-(7-carbamoyl-2-quinolinyl)pyridine derivatives 3a-e.

Compound		Salt[a]	mp (°C)[b]	Yield[c] %
1a	Beige crystals	2 $(COOH)_2$	> 260	59
1c	Beige crystals	2 $(COOH)_2$	> 260	67
1d	Orange crystals	4 $(COOH)_2$	243-245	71
1f	Orange crystals	4 $(COOH)_2$	255-257	64
1g	Beige crystals	2 $(COOH)_2$	> 260	73
1i	Orange crystals	2 $(COOH)_2$	> 260	66
1k	Beige crystals	2 $(COOH)_2$	> 260	70
1n	Beige crystals	2 $(COOH)_2$	> 260	54
2a	Beige crystals	2 $(COOH)_2$	> 260	51
2b	Beige crystals	2 $(COOH)_2$	> 260	74
2c	Beige crystals	4 $(COOH)_2$	> 260	63
2d	Beige crystals	2 $(COOH)_2$	> 260	57
2e	Dark-red crystals	2 $(COOH)_2$	> 260	69
2f	Beige crystals	4 $(COOH)_2$	> 260	57
2g	Beige crystals	2 $(COOH)_2$	> 260	72
3a	Beige crystals	2 $(COOH)_2$	> 260	78
3b	Beige crystals	4 $(COOH)_2$	197-199	63
3c	Beige crystals	2 $(COOH)_2$	254-256	47
3d	Beige crystals	2 $(COOH)_2$	259-261	65
3e	Beige crystals	2 $(COOH)_2$	215-217	52

Table 1: Physical properties of diquinolinyl-pyridines 1-3.

[a] The stoichiometry and composition of the salts were determined by elemental analyses and obtained values were within ±0.4% of the theoretical values.

[b] Crystallization solvent: 2-PrOH–H_2O.

[c] The yields only included the conversions into the ammonium oxalates.

Compound	*P. falciparum* strains IC_{50} values (µM)[a]		*L. donovani* IC_{50} values (µM)[b]	*Trypanosoma brucei brucei* IC_{50} values (µM)[c]	Cytotoxicity to HepG2 cells CC_{50} values (µM)[d]
	W2	3D7		Trypanos AnTat 1.9	
CQ[e]	0.40 ± 0.04	0.11 ± 0.01	n.d.[h]	n.d.[h]	30
MQ[e]	0.016 ± 0.002	0.06 ± 0.003	n.d.[h]	n.d.[h]	n.d.[h]
Pentamidine[f]	n.d.[h]	n.d.[h]	5.5 ± 0.8	0.0002 ± 0.00006	2.3 ± 0.5
Amphotericin B[f]	n.d.[h]	n.d.[h]	0.1 ± 0.04	n.d.[h]	8.8 ± 0.6
Suramine[g]	n.d.[h]	n.d.[h]	n.d.[h]	0.03 ± 0.003	n.d.[h]
Fexinidazole[g]	n.d.[h]	n.d.[h]	n.d.[h]	0.59 ± 0.039	n.d.[h]
Eflornithine[g]	n.d.[h]	n.d.[h]	n.d.[h]	15.19 ± 0.64	n.d.[h]
Doxorubicin	n.d.[h]	n.d.[h]	n.d.[h]	n.d.[h]	0.06 ± 0.02

1a	0.20 ± 0.01	0.38 ± 0.04	> 10	0.14 ± 0.03	2.03 ± 0.60
1b	0.18 ± 0.02	2.31 ± 0.21	> 10	0.84 ± 0.19	5.24 ± 1.10
1c	n.d.[h]	1.26 ± 0.34	> 10	1.54 ± 0.24	6.61 ± 2.75
1d	2.02 ± 0.20	0.91 ± 0.12	> 10	1.18 ± 0.08	n.d.[h]
1e	0.08 ± 0.01	0.60 ± 0.04	> 10	0.77 ± 0.01	5.88 ± 1.20
1f	n.d.[h]	0.23 ± 0.04	> 10	1.77 ± 0.18	3.09 ± 1.62
1g	2.00 ± 0.29	> 40	> 10	> 200	8.71 ± 0.11
1h	0.57 ± 0.06	1.29 ± 0.15	> 10	1.24 ± 0.11	2.20 ± 0.30
1i	n.d.[h]	0.22 ± 0.03	> 10	0.14 ± 0.02	3.39 ± 1.91
1j	0.32 ± 0.01	1.03 ± 0.06	> 10	0.18 ± 0.03	1.95 ± 0.60
1k	n.d.[h]	0.39 ± 0.04	> 10	0.75 ± 1.13	1.07 ± 0.15
1l	n.d.[h]	0.23 ± 0.05	> 10	0.64 ± 0.09	1.19 ± 0.15
1m	n.d.[h]	15.26 ± 3.23	> 10	18.79 ± 5.82	44.32 ± 9.50
1n	> 40	0.09 ± 0.01	> 10	> 50	n.d.[h]
2a	2.73 ± 0.17	2.51 ± 0.32	> 10	0.34 ± 0.05	3.88 ± 0.74
2b	1.66 ± 0.19	2.71 ± 0.78	> 10	1.14 ± 0.05	6.79 ± 1.85
2c	0.49 ± 0.06	1.53 ± 0.39	> 10	0.10 ± 0.01	7.59 ± 2.90
2d	0.33 ± 0.04	0.47 ± 0.10	> 10	0.25 ± 0.03	4.82 ± 1.80
2e	0.94 ± 0.10	1.48 ± 0.37	> 10	0.83 ± 0.09	6.66 ± 1.43
2f	2.54 ± 0.57	3.97 ± 0.32	> 10	6.11 ± 0.79	15.17 ± 1.53
2g	n.d.[h]	n.d.[h]	n.d.[h]	0.30 ± 0.08	n.d.[h]
3a	1.87 ± 0.27	6.29 ± 0.86	> 10	1.79 ± 0.33	11.44 ± 3.96
3b	0.60 ± 0.08	0.29 ± 0.04	> 10	0.16 ± 0.01	6.23 ± 1.68
3c	0.52 ± 0.05	1.20 ± 0.19	> 10	0.13 ± 0.03	3.66 ± 0.36
3d	1.29 ± 0.15	2.83 ± 0.49	> 10	0.61 ± 0.09	7.02 ± 1.90
3e	> 40	1.20 ± 0.10	> 10	0.43 ± 0.05	n.d.[h]

Table 2: *In vitro* sensitivity of *P. falciparum*, *L. donovani* and *T. brucei brucei* strains to compounds 1-3 and cytotoxicity of these compounds in HepG2 cells.

[a] Values were measured against CQ-resistant and MQ-sensitive strain W2 and the CQ-sensitive and MQ-resistant strain 3D7.

[b] IC_{50} values were measured against the promastigotes of *Leishmania donovani* strain. The IC_{50} (µM) values correspond to the means +/- standard deviations from 3 independent experiments.

[c] IC_{50} values were measured against the slender bloodstream trypomastigotes of *Trypanosoma brucei brucei* AnTat 1.9 strain. The IC_{50} (µM) values correspond to the means +/- standard deviations from 3 independent experiments with each concentration tested in duplicate in all experiments.

[d] CC_{50} values were measured against HepG2 cells. The CC_{50} (µM) values correspond to the means +/- standard deviations from 3 independent experiments.

[e] CQ and MQ were used as antiplasmodial compounds of reference.

[f] Pentamidine and amphotericin B were used as antileishmanial compounds of reference.

[g] Suramine, pentamidine, fexinidazole and eflornithine were used as antitrypanosomal compounds of reference.

[h] n.d.: not done.

incubation with *P. falciparum* CQ-resistant strain W2 (IC_{50} CQ = 0.40 µM, IC_{50} MQ = 0.016 µM) and the strain 3D7, which is CQ sensitive and which has decreased sensitivity to MQ (IC_{50} CQ = 0.11 µM, MQ = 0.06 µM). As shown in Table 2, these new 2,6-di-(carbamoyl-2-quinolinyl)pyridine derivatives showed IC_{50} values between 0.08 and 2.73 µM against W2, and between 0.09 and 15.26 µM against the 3D7 *P. falciparum* strains for the bioactive compounds.

Against the W2 strain, a *P. falciparum* CQ-resistant strain, 2,2'-(pyridine-2,6-diyl)bis(N-(3-(4-methylpiperazin-1-yl)propyl) quinoline-4-carboxamide)1e was found to be the most active with an IC_{50} of 0.08 µM. In the sub-series diquinolinyl-pyridine 1a-n, in which the derivatives were substituted by various aminoalkyl-carboxamide functions at position 4 of the quinoline moities, compounds 1b, 1e and 1h bearing C_3 side chains were found more active with IC_{50} of 0.18, 0.08 and 0.57 µM in comparison with their C_2 analogues 1a, 1d and 1g (IC_{50} =0.20, 2.02 and 2.00 µM, respectively).

For compounds 2a-g substituted by the different aminoalkyl-carboxamide functions at position 6 of the quinoline rings, those bearing two cyclic aminopropylcarboxamide functions in their structure, such as 4-methylpiperazinyl-, piperidinyl- or pyrrolidinylpropylcarboxamide (respectively compounds 2c, 2d and 2e), displayed better activity than the none cyclic aminopropylcarboxamide ones substituted with (dimethylamino) alkylcarboxamide (2a-b) or 3-((3-(dimethylamino)propyl)amino) propylcarboxamide (compound 1f) (IC_{50} ranging from 0.33 to 0.94 µM for 2c, 2d and 2e versus 1.66-2.73 µM for 2a-b. A similar observation could be noticed for the diquinolinyl-pyridines 3 substituted by two aminopropylcarboxamide side chains at position 7 on both quinoline moieties; i.e. IC_{50} of 0.60, 0.52 and 1.29 µM for cyclic aminopropylcarboxamide derivatives 3b-d in comparison with IC_{50} of 1.87 µM for 3-(dimethylamino)propylcarboxamide 3a. In terms of structure-activities relationships, we could also notice that each homologue substituted by the two aminopropyl-carboxamide functions at position 4 of the quinoline moities were found generally more active against the W2 strain than their respective analogues substituted in position 6, themselves more efficient than those with the same substituants in the 7 quinoline position. For example, 2,2'-(pyridine-2,6-diyl)bis(N-(3-(4-methylpiperazin-1-yl)propyl)quinoline-4-carboxamide) 1e was significantly more active (IC_{50} = 0.08 µM) than 2,2'-(pyridine-2,6-diyl)bis(N-(3-(4-methylpiperazin-1-yl)propyl)quinoline-6-carboxamide) 2c and 2,2'-(pyridine-2,6-diyl)bis(N-(3-(4-methylpiperazin-1-yl)propyl) quinoline-7-carboxamide) 3b (IC_{50} = 0.49 and 0.60 µM, respectively for these two bioactive derivatives 2c and 3b). The same type of remark could also be done for the compound 1b versus 2b then 3a; i.e. IC_{50} = 0.18 µM for derivative 1b compared to 1.66 and 1.87 µM for 2b and 3a, just like derivatives 1j versus 2d and 3c.

Against the CQ-sensitive strain 3D7, the 2,2'-(pyridine-2,6-diyl) bis(N-(3-(1H-imidazol-1-yl)propyl)quinoline-4-carboxamide) 1n was found the most potent antiplasmodial compound with an IC_{50} of 0.09 µM. This is very similar to IC_{50} values of the two reference drugs, CQ and MQ (IC_{50} = 0.11 and 0.06 µM, respectively). In each of the three sub-series (the two carboxamide functions in positions 4, 6 or 7 of the quinoline nuclei), compounds bearing (dimethylamino)alkylcarboxamide and 3-((3-(dimethylamino) propyl)amino)propylcarboxamide, diquinolinyl-pyridines 1b-c, 1m, 2a-b, 2f and 3a, showed lower antiparasitic activities (IC_{50} ranging from 1.26 to 15.26 µM) than derivatives bearing cyclic aminoalkylcarboxamide groups (1d-f, 1h-l, 1n, 2c-e, 3b-e with IC_{50} ranging from 0.09 to 2.83 µM), excepted for compound 1a for which an interesting antimalarial activity was observed (IC_{50} = 0.38 µM).

In vitro antileishmanial activity against promastigote forms

In order to better understand the biological profile of our novel 2,6-di-(carbamoyl-2-quinolinyl)pyridine derivatives 1-3, some complementary antiparasitic analyses were also performed. Notably, *P. falciparum* belongs to the coccidian protozoan parasite family. Therefore, their *in vitro* activity against protozoan parasite *L. donovani* was considered (Table 2). The reference drugs amphotericin B and pentamidine had IC_{50} values of 0.10 µM and 5.50 µM, respectively, against *L. donovani*. None of our new derivatives showed antileishmanial activity (all IC_{50} values > 10 µM).

In vitro activity against Trypanosoma brucei brucei

Our synthesized 2,6-di-(carbamoyl-2-quinolinyl)pyridine derivatives 1-3 were then evaluated against *T. brucei brucei*. Pentamidine, suramine, fexinidazole, and eflornithine were also used as reference compounds. These antiprotozoal data are presented in Table 2. Most of these novel diquinolinyl-pyridines

1-3 were active against *T. brucei brucei* with IC_{50} values ranging from 0.10 to 18.79 µM; but most of these derivatives showed an antitrypanosomal activity around the µM value. The best efficacy against the *T. brucei brucei* strain was observed with 2,6-di-(6-carbamoyl-2-quinolinyl)pyridine 2c with an IC_{50} of 0.10 µM. Against this parasite, it also seems interesting to note that certain compounds bearing linear aminopropylcarboxamide or aminobutylcarboxamide functions (compounds 1c, 1m, 2b, 2f and 3a) were found less active than those with two cyclic aminopropylcarboxamides (1d-f, 1h-l, 2c-e, 2g and 3b-e) : IC_{50} = 1.54-18.79 µM for 1c, 1m, 2b, 2f and 3a compared to IC_{50} = 0.10-1.77 µM for 1d-f, 1h-l, 2c-e, 2g and 3b-e. However, compound 1a bearing two linear aminoethylcarboxamide groups showed a good antitrypanosomal activity (IC_{50} = 0.14 µM).

Cytotoxicity and selectivity index

In order to calculate the selectivity of action, the cytotoxicities of these novel synthesized antiparasitic 2,6-di-(carbamoyl-2-quinolinyl)pyridine derivatives 1-3 were evaluated *in vitro* in the human cell line HepG2, which is a commonly used human-derived hepatocarcinoma cell line, and express many hepatocyte-specific metabolic enzymes. The aim was to evaluate the impact of metabolic activation of the new tested compounds on cell viability. The cytotoxic concentrations 50% (CC_{50}) were determined, and selectivity indexes (SI), defined as the ratios of cytotoxic to antiparasitic activities (SI = CC_{50}/IC_{50}) were then calculated. The results of cytotoxicity assays and their respective associated SI values were presented in Table 3. These novel diquinolinyl-pyridines 1-3 that were noticed active against the different parasites showed significant cytotoxicity against the HepG2 cells with CC_{50} values ranging from 1.07 to 44.32 µM.

For the malaria W2 strain, the SIs were found between 1.42 and 73.5. The SIs ranged from 1.70 to 21.48 for the CQ sensitive strain 3D7. Analyses of the SI values identified 2,6-di-(carbamoyl-2-quinolinyl)pyridine 1e as potential interesting derivative with SI of 73.5 for the CQ resistant strain W2 strain, and also diquinolinyl-pyridines 1i and 3b with SI of 15.41 and 21.48 for the 3D7 strain, respectively. Against the *T. brucei brucei* strain, the two diquinolinyl-pyridine derivatives 2c and 3b showed SI of 75.9 and 38.94, respectively. These promising and interesting selectivity indexes values could indicate that these novel aza polyheterocyclic compounds warrant further investigations into their potential use as antiparasitic compounds.

Compound	Selectivity Index[a]			
	HepG2/ W2	HepG2/ 3D7	HepG2/*L. donovani*	HepG2/ Tryp.
CQ	75	272	n.d.[b]	n.d.[b]
Pentamidine	n.d.[b]	n.d.[b]	0.42	11500
Amphotericin B	n.d.[b]	n.d.[b]	88.0	n.d.[b]
1a	15.61	5.34	n.d.[b]	14.5
1b	29.11	2.27	n.d.[b]	6.24
1c	n.d.[b]	5.25	n.d.[b]	4.29
1d	n.d.[b]	n.d.[b]	n.d.[b]	n.d.[b]
1e	73.5	9.80	n.d.[b]	7.64
1f	n.d.[b]	13.43	n.d.[b]	1.74
1g	4.36	n.d.[b]	n.d.[b]	n.d.[b]
1h	3.86	1.70	n.d.[b]	1.77
1i	n.d.[b]	15.41	n.d.[b]	24.21
1j	6.09	1.89	n.d.[b]	10.83
1k	n.d.[b]	2.74	n.d.[b]	1.42
1l	n.d.[b]	5.17	n.d.[b]	1.86
1m	n.d.[b]	2.90	n.d.[b]	2.36
1n	n.d.[b]	n.d.[b]	n.d.[b]	n.d.[b]
2a	1.42	1.55	n.d.[b]	11.41
2b	4.09	2.50	n.d.[b]	5.96
2c	15.49	4.96	n.d.[b]	75.9
2d	14.61	10.26	n.d.[b]	19.28
2e	7.09	4.50	n.d.[b]	8.02
2f	5.97	3.82	n.d.[b]	2.48
2g	n.d.[b]	n.d.[b]	n.d.[b]	n.d.[b]
3a	6.12	1.82	n.d.[b]	6.39
3b	10.38	21.48	n.d.[b]	38.94
3c	7.04	3.05	n.d.[b]	28.15
3d	5.44	2.48	n.d.[b]	11.51
3e	n.d.[b]	n.d.[b]	n.d.[b]	n.d.[b]

Table 3: Selectivity indexes of 2,6-di-(carbamoyl-2-quinolinyl) pyridine derivatives 1-3.

[a] SI was defined as the ratio between the CC_{50} value on the HepG2 cells and the IC_{50} value against the *P. falciparum* W2 or 3D7 or *Trypanosoma brucei brucei* strains.

[b] n.d.: not done.

FRET-melting experiments

The telomeres of the parasites *P. falciparum* and Trypanosoma have been previously described as potential targets for this kind of heterocyclic aza derivatives, consequently have also investigated the stabilization of the *P. falciparum* telomeric or *T. brucei brucei* chromosomic G-quadruplexes by a panel of our bioactive antiprotozoal derivatives 1a-c, 1g-j, 1l-m, 2c and 3b-c through a FRET melting assays. To determine the degree to which these novel 2,6-di-(carbamoyl-2-quinolinyl)pyridine derivatives stabilize the G-quadruplexes formed by oligonucleotides with *P. falciparum* or *T. brucei brucei* as well as human telomeric sequences, a FRET melting assay was used. Thus, two fluorescently labeled *P. falciparum* telomeric, one *T. brucei brucei* chromosomic sequences (FPf1T, FPf8T and FtrypBT) and one human telomeric sequence (F21T) were used. In addition, a FRET melting assay was realized using a duplex control sequence, FdxT to probe the G4 selectivity of our new selected ligands over duplex DNA, For comparison, we evaluated reference G4 ligand PhenDC3 and the antimalarial reference drugs CQ and MQ. To enable comparison of selectivities, the difference (DTm) between the Tm of the G-quadruplex formed by FPf1T, FPf8T, FtrypBT (FEBR1T), F21T or FdxT in the presence or absence of each selected ligand was calculated. These DTm values are presented in Table 4. For these new synthesized and selected ligands 1a-c, 1g-j, 1l-m, 2c and 3b-c, the DTm values on the G-quadruplex ranged from 2.0 to 30.6 °C at 5 μM ligand concentration.

Figure 2: Stabilization specificity profile of 1a-c, 1g-h, 1j, 1l and 1m (5 μM) toward the FPf1T, FPf8T, F21T and FdxT G4 oligonucleotides. The difference in Tm in presence and absence of ligand; ΔTm, in °C is plotted for each sequence. Three quadruplexes and one duplex (FdxT) were tested.

Compound	DT_m (°C)[a]		DT_m (°C)[a]		DT_m (°C)[a]	DT_m (°C)[a]		DT_m (°C)[a]	
	FPf1T		FPf8T		FtrypBT	F21T		FdxT	
PhenDC3	24.6	± 0.1	24.7	± 0.2	19.2 ± 0.2	26.3	± 0.1	0.1	± 0.2
CQ	1.9	± 0.1	2.4	± 1.2	n.d.[b]	2.4	± 1.1	n.d.[b]	
MQ	3.1	± 0.5	6.6	± 2.3	n.d.[b]	2.6	± 0.5	n.d.[b]	
1a	14.6	± 0.4	15.3	± 1.2	8.7 ± 0.3	15.6	± 1.1	1.0	± 0.7
1b	18.2	± 1.4	18.8	± 1.1	10.2 ± 0.5	19.8	± 0.3	0.5	± 0.1
1c	12.4	± 0.8	12.9	± 0.8	n.d.[b]	14.9	± 0.6	0.6	± 0.2
1g	2.9	± 0.6	4.1	± 1.0	n.d.[b]	3.3	± 0.3	0.4	± 0.1
1h	2.2	± 0.6	2.5	± 0.5	n.d.[b]	2.0	± 0.3	0.7	± 0.3
1i		n.d.[b]		n.d.[b]	7.1 ± 0.1	8.1	± 1.0	n.d.[b]	
1j	20.1	± 0.9	15.6	± 0.7	8.6 ± 1.2	18.9	± 1.3	0.7	± 0.1
1l	17.5	± 1.2	17.3	± 0.8	n.d.[b]	17.7	± 1.4	0.9	± 0.1
1m	25.4	± 1.4	27.3	± 1.1	n.d.[b]	23.5	± 0.9	1.1	± 0.6
2c		n.d.[b]		n.d.[b]	22.9 ± 0.4	26.4 ± 0.1			n.d.[b]
3b		n.d.[b]		n.d.[b]	24.4 ± 0.1	30.6 ± 0.6			n.d.[b]
3c		n.d.[b]		n.d.[b]	26.3 ± 1.4	28.2 ± 0.2			n.d.[b]

Table 4: FRET-melting values for the selected compounds 1a-c, 1g-j, 1l-m, 2c and 3b-c with FPf1T, FPf8T, FtrypBT, F21T and FdxT in K^+ conditions at 5 μM.

[a] DT_m of FPf1T, FPf8T, FtrypBT, F21T and FdxT (0.2 μM) were recorded in 10 mM lithium cacodylate (pH 7.2), 10 mM KCl, 90mM LiCl. PhenDC3 was tested at 0.5 μM, whereas CQ and MF at 1 μM. Error margins correspond to SD of three replicates.

[b] n.d.: not determined.

Among our tested compounds, the best 2,6-di-(carbamoyl-2-quinolinyl)pyridine ligand that stabilize the two Plasmodium G-quadruplexes sequences was compound 1m (Table 4). Thus, the best di-nitrogen heterocyclic ligand which stabilize the two parasitic FPf1T, FPf8T and the human F21T G-quadruplexes sequences was the 2,2'-(pyridine-2,6-diyl)bis(N-((substituted-amino)alkyl)quinoline-4-carboxamide) 1m with DTm values ranging from 23.5 to 27.3°C. This diquinolinyl-pyridine ligand 1m was found to show the same stabilization level in comparison with the reference PhenDC3 ligand. The other selected compounds 1a-c 1j, and 1l, also exhibited interesting stabilization profile for all the G4 sequences (DTm = 12.4-20.1 °C on FPf1T; and DTm = 12.9-18.8°C on FPf8T), however compounds 1g-h, both substituted by morpholinoalkyl chains, surprinsingly displayed lower stabilization on the two parasitic FPf1T/FPf8T and human F21T sequences than their other homologues 1 with DTm values ranging from 2.2 to 4.1 °C (Figure 2). An other observation showed that our tested compounds 1 displayed a better stabilization profile for both the *P. falciparum* telomeric sequences than the *T. brucei brucei* chromosomic G-quadruplex. In addition, it could be also noticed that the substitution of the two aminoalkylcarboxamide functions in position 6 and 7 of the quinoline rings (compounds 2c and 3b-c) showed higher DTm values on the *T. brucei brucei* G-quadruplex in comparison with their homologues 1 for which the same functions were substituted in positions 4 of the aza heterocyclic skeletons; i.e. DTm = 22.9-26.3 °C for 2c and 3b-c versus DTm = 7.1-10.2 °C for 1a-b and 1i-j. The FRET assays also showed there was no binding to duplex DNA sequence.

Conclusion

In the present research report, we described the design, synthesis, the antiparasitic activities, and the *in vitro* cytotoxicity toward human cells of a new series of 2,6-di-(carbamoyl-2-quinolinyl)pyridine derivatives 1-3. These novel compounds were tested for their *in vitro* antiprotozoal activity toward the CQ-resistant W2 and CQ-sensitive 3D7 *P. falciparum* strains, the promastigote form of *L. donovani*, and a *T. brucei brucei* strain. Among these new synthesized diquinolinyl-pyridines, a few have potential interest as antiplasmodial lead derivatives with IC_{50} values in the sub and µM range against *P. falciparum*. Unfortunately, none of our compounds showed activity against the promastigote forms of *L. donovani*. In addition, their antiprotozoal activity spectrum using a *T. brucei brucei* strain showed an antitrypanosomal activity around the µM value, which warrant further investigation. Moreover, when the *in vitro* cytotoxicity of these new diquinolinyl-pyridines was also assessed using human HepG2 cells we have identified compound 1e with an index of selectivity of 73.5 for the CQ-resistant W2; and derivative 2c was also identified as the most potent trypanosomal candidate with selectivity index (SI) of 75.9 on *Trypanosoma brucei brucei* strain. In conclusion, this new substituted 2,6-di-(carbamoyl-2-quinolinyl)pyridine scaffold could open the way to new valuable medicinal chemistry lead compounds in the antiprotozoal domain.

Conflict of Interest

The authors report no conflicts of interest. The authors alone are responsible for the content and writing of the paper.

Acknowledgments

The authors would like to thank Pr. Philippe Grellier, department RDDM at Muséum National d'Histoire Naturelle (Paris, France), for providing generously the 3D7 and W2 *P. falciparum* strains.

Bibliography

1. World malaria report 2022 (2023).
2. WHO Guidelines for malaria hosted on the MAGICapp online platform (2023).
3. WHO Neglected tropical diseases (2023).
4. WHO Ending the neglect to attain the sustainable development goals: a rationale for continued investment in tackling neglected tropical diseases 2021-2030 (2023).
5. Dola VR., *et al.* «Synthesis and Evaluation of Chirally Defined Side Chain Variants of 7-Chloro-4-Aminoquinoline To Overcome Drug Resistance in Malaria Chemotherapy". *Antimicrobial Agents and Chemotherapy* 61 (2017): e01152-16.
6. Manohar S., *et al.* "4-Aminoquinoline based molecular hybrids as antimalarials: an overview". *Current Topics in Medicinal Chemistry* 14 (2014): 1706-1733.
7. Deshpande S., *et al.* "4-aminoquinolines: An Overview of Antimalarial Chemotherapy". *Medicinal Chemistry* 6 (2016): 1.
8. Kumar S., *et al.* "Recent advances in novel heterocyclic scaffolds for the treatment of drug-resistant malaria". *Journal of Enzyme Inhibition and Medicinal Chemistry* 31 (2016): 173-186.

9. Van de Walle T., *et al.* "Recent contributions of quinolines to antimalarial and anticancer drug discovery research". *European Journal of Medicinal Chemistry* 226 (2021): 113865.

10. Goyal A., *et al.* "Spotlight on 4-substituted quinolines as potential anti-infective agents: Journey beyond chloroquine". *Archiv der Pharmazie (Weinheim)* 356 (2023): e2200361.

11. Hochegger P., *et al.* "New derivatives of quinoline-4-carboxylic acid with antiplasmodial activity". *Bioorganic and Medicinal Chemistry* 25 (2017): 2251-2259.

12. Baragaña B., *et al.* "A novel multiple-stage antimalarial agent that inhibits protein synthesis". *Nature* 522 (2015): 315-320.

13. Pandya KM., *et al.* "Development of Antimicrobial, Antimalarial and Antitubercular Compounds Based on a Quinoline-Pyrazole Clubbed Scaffold Derived via Doebner Reaction". *Chemistry Africa* 3 (2020): 89-98.

14. Guillon J., *et al.* "Synthesis, antimalarial activity, and molecular modeling of new pyrrolo[1,2-*a*]quinoxalines, bispyrrolo[1,2-*a*] quinoxalines, bispyrido[3,2-*e*]pyrrolo[1,2-*a*]pyrazines, and bispyrrolo[1,2-*a*]thieno[3,2-*e*]pyrazines". *Journal of Medicinal Chemistry* 47 (2004): 1997-2009.

15. Guillon J., *et al.* "Synthesis and antiprotozoal evaluation of new 2,9-bis[(pyridinylalkylaminomethyl)phenyl]-1,10-phenanthroline derivatives by targeting G-quadruplex, an interesting pharmacophore against drug efflux". *Acta Scientific Pharmaceutical Sciences* 7 (2023): 50-65.

16. Guillon J., *et al.* "Design, synthesis and antimalarial activity of novel bis{*N*-[(pyrrolo[1,2-*a*]quinoxalin-4-yl)benzyl]-3-aminopropyl}amine derivatives". *Journal of Enzyme Inhibition and Medicinal Chemistry* 32 (2017): 547-563.

17. Jonet A., *et al.* "Synthesis and Antimalarial Activity of New Enantiopure Aminoalcoholpyrrolo[1,2-*a*]quinoxalines". *Medicinal Chemistry* 14 (2018): 293-303.

18. Guillon J., *et al.* "Design, synthesis, and antiprotozoal evaluation of new 2,4-bis[(substituted-aminomethyl) phenyl]quinoline, 1,3-bis[(substituted-aminomethyl)phenyl] isoquinoline and 2,4-bis[(substituted-aminomethyl)phenyl] quinazoline derivatives". *Journal of Enzyme Inhibition and Medicinal Chemistry* 35 (2020): 432-459.

19. Dassonville-Klimpt A., *et al.* "Design, synthesis, and characterization of novel aminoalcohol quinolines with strong *in vitro* antimalarial activity". *European Journal of Medicinal Chemistry* 228 (2022): 113981.

20. Guillon J., *et al.* "Design, synthesis, and antiprotozoal evaluation of new 2,9-bis[(substituted-aminomethyl)phenyl]-1,10-phenanthroline derivatives". *Chemical Biology and Drug Design* 91 (2018): 974-995.

21. Calvo EP., *et al.* "G-Quadruplex ligands: Potent inhibitors of telomerase activity and cell proliferation in *Plasmodium falciparum"*. *Molecular and Biochemical Parasitology* 207 (2016): 207, 33-38.

22. Tidwell RR., *et al.* "Dicationic compounds which selectively recognize G-quadruplex DNA". (2007): 1792613A2.

23. Leeder WM., *et al.* "Multiple G-quartet structures in pre-edited mRNAs suggest evolutionary driving force for RNA editing in trypanosomes". *Scientific Reports* 6 (2016): 29810.

24. Lombrana R., *et al.* "Transcriptionally Driven DNA Replication Program of the Human Parasite Leishmania major". *Cell Reports* 16 (2016): 1774-1786.

25. Bottius E., *et al.* "*Plasmodium falciparum* Telomerase: De Novo Telomere Addition to Telomeric and Nontelomeric Sequences and Role in Chromosome Healing". *Molecular and Cellular Biology* 18 (1998): 919-925.

26. Raj DK., *et al.* "Identification of telomerase activity in gametocytes of *Plasmodium falciparum*". *Biochemical and Biophysical Research Communications* 309 (2003): 685-688.

27. Das RN., *et al.* "Design, synthesis and biological evaluation of new substituted diquinolinyl-pyridine ligands as anticancer agents by targeting G-quadruplex". *Molecules* 23 (2018): 81.

28. Desjardins RE., *et al.* "Quantitative assessment of antimalarial activity *in vitro* by a semiautomated microdilution technique". *Antimicrobial Agents and Chemotherapy* 16 (1979): 710-718.

29. Bennett TN., *et al.* "Novel, Rapid, and Inexpensive Cell-Based Quantification of Antimalarial Drug Efficacy". *Antimicrobial Agents and Chemotherapy* 48 (2004): 1807-1810.

30. Bacon DJ., *et al.* "Comparison of a SYBR Green I-Based Assay with a Histidine-Rich Protein II Enzyme-Linked Immunosorbent Assay for *In Vitro* Antimalarial Drug Efficacy Testing and Application to Clinical Isolates". *Antimicrobial Agents and Chemotherapy* 51 (2007): 1172-1178.

31. Kaddouri H., *et al.* "Assessment of the Drug Susceptibility of *Plasmodium falciparum* Clinical Isolates from Africa by Using a *Plasmodium* Lactate Dehydrogenase Immunodetection Assay and an Inhibitory Maximum Effect Model for Precise Measurement of the 50-Percent Inhibitory Concentration". *Antimicrobial Agents and Chemotherapy* 50 (2006): 3343-3349.

32. Mosmann T. "Rapid colorimetric assay for cellular growth and survival: application to proliferation and cytotoxicity assays". *Journal of Immunological Methods* 65 (1983): 55-63.

33. Emami SA., *et al.* "Inhibitory Activity of Eleven *Artemisia* Species from Iran against *Leishmania* Major Parasites". *Iranian Journal of Basic Medical Sciences* 15 (2012): 807-811.

34. Räz B., *et al.* "The Alamar Blue assay to determine drug sensitivity of African trypanosomes (*T.b. rhodesiense* and *T.b. gambiense*) *in vitro*". *Acta Tropica* 68 (1997): 139-147.

35. Baltz T., *et al.* "Cultivation in a semi-defined medium of animal infective forms of *Trypanosoma brucei*, *T. equiperdum*, *T. evansi*, *T. rhodesiense* and *T. gambiense*". *EMBO Journal* 4 (1985): 1273-1277.

36. De Cian A., *et al.* "Fluorescence-based melting assays for studying quadruplex ligands". *Methods* 42 (2007): 183-195.

37. Buu-Hoï *et al.* "Nitrogen heterocyclic analogs of polyaryls". *Journal of Heterocyclic Chemistry* 2 (1965): 7-10.

38. Marin I., *et al.* "Homoleptic and heteroleptic ruthenium(II) complexes based on 2,6-bis(quinolin-2-yl)pyridine ligands-multiple-charged-state modules for potential density memory storage". *European Journal of Inorganic Chemistry* 5 (2015): 786-793.

39. Li C., *et al.* "Asymmetric Ruthenium-Catalyzed Hydrogenation of Terpyridine-Type *N*-Heteroarenes: Direct Access to Chiral Tridentate Nitrogen Ligands". *Organic Letters* 22 (2020): 6452-6457.